Earth's Future

RESEARCH ARTICLE
10.1029/2021EF002187

Special Section:
Modeling MultiSector Dynamics to Inform Adaptive Pathways

Technology Pathways Could Help Drive the U.S. West Coast Grid's Exposure to Hydrometeorological Uncertainty

Jacob Wessel[1], Jordan D. Kern[2], Nathalie Voisin[3,4], Konstantinos Oikonomou[4], and Jannik Haas[5]

[1]Department of Civil, Construction, and Environmental Engineering, North Carolina State University, Raleigh, NC, USA, [2]Department of Forestry and Environmental Resources, North Carolina State University, Raleigh, NC, USA, [3]Pacific Northwest National Laboratory, Seattle, WA, USA, [4]Civil and Environmental Engineering Department, University of Washington, Seattle, WA, USA, [5]German Aerospace Center, Stuttgart, Germany

Abstract Previous studies investigating deep decarbonization of bulk electric power systems and wholesale electricity markets have not sufficiently explored how future grid pathways could affect the grid's vulnerability to hydrometeorological uncertainty on multiple timescales. Here, we employ a grid operations model and a large synthetic weather ensemble to "stress test" a range of future grid pathways for the U.S. West Coast developed by ReEDS, a well-known capacity planning model. Our results show that gradual changes in the underlying capacity mix from 2020 to 2050 can cause significant "re-ranking" of weather years in terms of annual wholesale electricity prices (with "good" years becoming bad, and vice versa). Nonetheless, we find the highest and lowest ranking price years in terms of average electricity price remain mostly tied to extremes in hydropower availability (streamflow) and load (summer temperatures), with the strongest sensitivities related to drought. Seasonal dynamics seen today involving spring snowmelt and hot, dry summers remain well-defined out to 2050. In California, future supply shortfalls in our model are concentrated in the evening and occur mostly during periods of high temperature anomalies in late summer months and in late winter; in the Pacific Northwest, supply shortfalls are much more strongly tied to negative streamflow anomalies. Under our more robust sampling of stationary hydrometeorological uncertainty, we also find that the ratio of dis-patchable thermal (i.e., natural gas) capacity to wind and solar required to ensure grid reliability can differ significantly from values reported by ReEDS.

Plain Language Summary In this study we model how increased adoption of wind power, solar power, batteries and electric vehicles could alter the U.S. West Coast grid's exposure to weather uncertainty. Our results show that as the mix of technologies used on the grid changes from 2020 to 2050, it will cause a "re-ranking" of weather years (with "good" years capable of becoming "bad" and vice versa). For example, years with low wind speeds generally become more concerning (marked by comparatively high prices) as installed wind power increases. Nonetheless, the highest and lowest price years remain most strongly tied to extremes in hydropower availability (streamflow) and electricity demand (summer air temperatures) even out to 2050. In California, supply shortfalls are concentrated in the evening during periods of anomalously high temperatures in late summer and late winter; in the Pacific Northwest, supply shortfalls are most strongly tied to negative streamflow anomalies. By subjecting various decarbonization scenarios to weather uncertainty, we also find that the amount of "firm" (natural gas) capacity needed to ensure reliability can differ significantly from values reported in a widely used capacity expansion model.

Key Points:

- Changing capacity mixes cause "re-ranking" of weather years in terms of annual price
- Nonetheless, the highest and lowest price years remain tied to extremes in hydropower production and load
- Capacity expansion models may misrepresent firm capacity needed under weather uncertainty

Supporting Information:

Supporting Information may be found in the online version of this article.

Correspondence to:

J. Wessel,
jawessel@ncsu.edu

Citation:

Wessel, J., Kern, J. D., Voisin, N., Oikonomou, K., & Haas, J. (2022). Technology pathways could help drive the U.S. West Coast grid's exposure to hydrometeorological uncertainty. *Earth's Future*, *10*, e2021EF002187. https://doi.org/10.1029/2021EF002187

Received 7 MAY 2021
Accepted 20 DEC 2021

1. Introduction

Many previous investigations have explored the wide-ranging effects of deep decarbonization of electric power systems on cost (including market prices), system reliability, and environmental performance (Haas et al., 2018; Kavalec et al., 2018; Li & Hedman, 2015; Mai et al., 2012; Steinberg et al., 2017; Sun et al., 2018; Woo et al., 2017). However, key questions remain unanswered, including the vulnerability of future grid configurations to uncertainty in hydrometeorological conditions, which strongly affects interactions between supply and demand (and thus price dynamics) in power markets (Tarroja et al., 2016).

Electricity demand fluctuates constantly, driven in large part by changes in heating and cooling demands, which are themselves driven by weather (air temperatures, wind speeds, and humidity) (Bain & Acker, 2018). Demand

must be balanced in real-time using installed generating capacity from a mix of technologies, many of which are influenced by hydrometeorological conditions. For example, streamflow dynamics govern the timing and availability of hydropower and the availability of cooling water at some thermal power plants. As a result, inter-annual and seasonal variability in hydrologic conditions can significantly alter power system costs, market prices, and emissions of carbon dioxide (CO_2) and other pollutants (Bain & Acker, 2018; Madani & Lund, 2010; Tarroja et al., 2016). Variable renewable energy production (i.e., wind and solar power) is similarly limited by solar irradiance and wind speeds, and fluctuations in these processes can affect prices and emissions, with the strongest effects typically observed on shorter (daily and hourly) timescales (Joskow, 2019; Seel et al., 2018; Staffell & Pfenninger, 2018; Wiser et al., 2017).

As installed wind and solar capacity increases, the grid's power supply is likely to become even more sensitive to fluctuations in wind speeds and solar irradiance. How this gradual, increased exposure to uncertainty in wind speeds and solar irradiance will combine with multi-scale variability in air temperatures and streamflows to affect grid performance remains an outstanding research question.

This question is particularly relevant for the West Coast region of the United States (U.S.), where California and Washington State both aim to meet 100% of their electricity demand from zero-carbon sources by 2045, while Oregon is aiming for 50% by 2040 (N.C. Clean Energy Technology Center, 2021). Without adequate planning, the West Coast power system's increased reliance on renewable energy may expose systems to potential supply shortfalls, if periods of low wind speeds coincide with periods of high demand (e.g., a heat wave). A recent example of this phenomenon are the rolling blackouts that occurred in California in summer 2020 (Roth, 2020). On the other hand, increased adoption of variable renewable energy may also create more frequent periods of "oversupply" on the grid, when the availability of renewable energy (in combination with "must run" resources like nuclear power) can eclipse demand, leading to forcible curtailment of renewables and negative wholesale prices (Bushnell & Novan, 2018; De Jonghe et al., 2011; Denholm et al., 2008). Already in California's wholesale electricity market, electricity prices regularly reach low (and even negative) levels when there is a glut of renewable energy on the grid (Trabish, 2017).

However, variable renewable energy is only one of several different new technologies that could reshape grid operations. Future grid configurations are also likely to include significantly higher levels of grid-scale battery storage and electric vehicles (Denholm et al., 2010; Mai et al., 2018a). These may also (indirectly) alter the grid's sensitivity to hydrometeorological uncertainty. For example, batteries would allow system operators to time-shift the use of wind and solar to hours in which demand and/or price is higher. In theory, the result would be less volatile intra-day price patterns and a lower need for other forms of structural redundancy (generation capacity and operating reserves) (Denholm et al., 2019; Mohsenian-Rad, 2016; Senjyu et al., 2007), and reduced curtailment of renewables during oversupply events (Bruninx & Delarue, 2017; Johnson et al., 2014).

Electric vehicle adoption has also been steadily increasing in the U.S especially in California (Nikolewski, 2019). As the shift towards widespread electrification of the transportation sector continues, the effects will be felt by grid operators, most notably in the form of altered aggregate hourly electricity demand from vehicle charging, including altered timing and magnitude of peak demand hours (Energy and Environmental Economics, Inc., 2014; Han et al., 2017). Electric vehicles thus represent a confounding variable that could exacerbate (or, depending on how they are deployed, help mitigate) the effects of hydrometeorological uncertainty on electricity prices, grid reliability, and CO_2 emissions.

As the West Coast grid continues to evolve, its physical and financial exposure to fluctuations in hydrometeorological conditions is likely to change as well, even without factoring in the anticipated effects of climate change. While there have been major efforts to explore power system and market dynamics under future grid configurations, including on the West Coast, few have adequately explored this system's exposure to stationary hydrometeorological uncertainty (Haas et al., 2018; Hadley & Tsvetkova, 2009; Li et al., 2016; Pereira et al., 2018). At the same time, most previous studies focused on grid impacts from hydrometeorological conditions do not consider how these sensitivities will change as the underlying technology mix evolves (Jordehi, 2018; Jurkovic et al., 2017).

Here, we explore how grid technology pathways (i.e., increasing levels of variable renewable energy, electric vehicles, and battery storage) could help drive the West Coast power system's exposure to hydrometeorological uncertainty. We couple an open-source power system simulation tool with methods for stochastically modeling

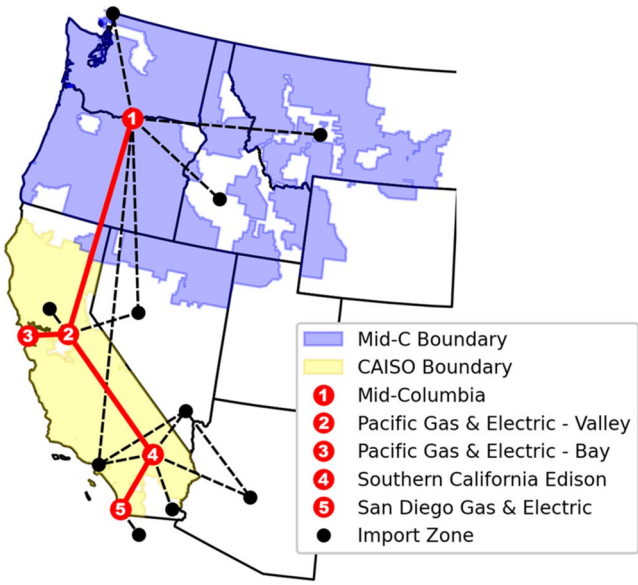

Figure 1. System topology of California and West Coast Power Systems model, showing the five modeled zones and boundaries of the two major systems. Power exchanges among modeled zones 2–5 are modeled mechanistically, while all other exchanges are trained on historical data (2008–2012) and modeled statistically.

the availability of hydropower, wind and solar power, and electricity demand, which take as inputs synthetically generated hydrometeorological time series. This allows us to capture impacts from 1-in-100 and even 1-in-1000-year statistical events that would not otherwise be discoverable within a limited historical data set. We explore a wide range of alternative grid technology pathways that vary principally in the degree and rate of uptake of renewable energy, electric vehicles, and energy storage, using scenarios developed by the Regional Energy Deployment System (ReEDS) capacity planning model (Brown et al., 2019). Results obtained by this study significantly improve knowledge regarding future hydrometeorological risks in bulk electric power systems, providing a roadmap that decision makers can use to understand how sensitivity to weather will evolve as a function of technology choices.

2. Methods

2.1. Power Systems Modeling

In order to simulate the operations of the U.S. West Coast bulk power system, we make use of the CAPOW (California and West Coast Power Systems) model, which was developed specifically to explore the impacts of hydrometeorological uncertainty on the performance of this regional grid (Su, Kern, Denaro, et al., 2020). CAPOW generates expanded synthetic records of hydrometeorological data and converts these to relevant power system inputs, which are then fed to multi-zone unit commitment and economic dispatch (UC/ED) problems that separately represent the operations of two major wholesale markets: the California Independent System Operator (CAISO) and the informal Mid-Columbia (Mid-C) covering the majority of the Pacific Northwest. As shown in Figure 1, the CAPOW model's topology consists of five zones connected by aggregated transmission lines. Zones 2–5 make up CAISO, while Zone 1 represents the informal Mid-C. Each zone has its own time-varying electricity demand and generation portfolio. Power flows among CAISO zones (2–5) are modeled mechanistically as decision variables. Power exchanges with outside regions outside the West Coast (as well as between the Mid-C and CAISO systems) are trained on historical data and modeled statistically on a daily time step. Inter-annual, seasonal, and sub-seasonal fluctuations in these interregional power flows are currently explainable in large part by zonal load and hydropower availability; in this study, we do not consider how these dynamics could change in the future as a function of technology adoption. Treating zonal power flows as decision variables in a single, global cost minimization objective for the entire model domain (i.e., CAISO and Mid-C) could in theory allow for zonal exchanges to change as a function of technology adoption. However, this approach is less capable of capturing observed dynamics in the current system, because in reality the Mid-C and CAISO markets are operated as distinct systems with a number of institutional practices preventing close coordination.

Instead, operations in each market are represented using a separate UC/ED formulated as an iterative, mixed-integer linear program. Each UC/ED is coded in Python using the Pyomo optimization package, and solved with Gurobi. Using a 48-hr operating horizon, each UC/ED solves for the minimum cost of meeting demand and operating reserves by first committing adequate flexible generation capacity and then dispatching the optimal amount by each committed generator on an hourly basis. To avoid the model having perfect foresight, only the first 24 hr of the operating horizon are saved from each model iteration, while the rest is discarded and the model shifts 24 hr into the future. This optimization is repeated until a full year is simulated, which takes approximately 10 hr (solving for approximately 220,000 decision variables) on North Carolina State University's high performance computing cluster.

2.2. Future Grid Pathways

We explore a range of potential future grid pathways in which installed grid technology mixes evolve through the year 2050. These pathways are the output of selected standard technology and policy trajectories produced by the National Renewable Energy Laboratory's Regional Energy Deployment System (ReEDS) capacity expansion

model (Brown et al., 2019; Cole et al., 2019). The ReEDS model iteratively solves three interdependent modules (supply, demand, and variable renewable energy) to reach a power system equilibrium at each future time step. These solutions plot the evolution of the U.S. electric power system over time, given a scenario-specific set of assumptions (e.g., technology and fuel costs). Additional information about the ReEDS capacity expansion model can be found in the Supporting Information S1. From the ReEDS model outputs, we collected the average annual load (in TWh) and installed generation capacity (in GW) for each technology, for each state in our study area, in five year "stages" ranging from 2020 to 2050. Five distinct technology pathways were considered: (a) a Midcase (reference pathway) projecting business-as-usual conditions (MID); (b) a High Electric Vehicle Adoption pathway (EV); (c) a Low Battery Storage Cost pathway (BAT); (d) a Low Renewable Energy Cost/High Natural Gas Price pathway (LOWRECOST); and (e) a High Renewable Energy Cost/Low Natural Gas Price pathway (HIGHRECOST). These technology pathways were chosen heuristically based on a desire to achieve cross-scenario diversity and to highlight specific emerging technologies. Each pathway was then simulated using the CAPOW model to explore the vulnerability of the West Coast power system to hydrometeorological uncertainty and extremes. In the remainder of this paper, we refer to each combination of pathway/stage as a "scenario". We explore 35 unique scenarios in all (5 ReEDS pathways x 7 stages [2020, 2025 … 2050]).

The main objective of this study is to explore the sensitivity of power market dynamics to increased penetration of renewable energy, regardless of the absolute size of the system as measured by average or peak load. Our intent is not to prescribe what will happen to this specific system in the future, but rather to take the current makeup of the system in question (large hydropower dependency and summer peaking load) and explore changes in its behavior that emerge under higher levels of variable renewable energy. This study does not include long-term population growth or climate change when constructing scenarios, both of which could impact the vulnerability of this particular system as it decarbonizes. While these impacts are critical, we first want to understand the sensitivity of the system to changes in technology before combining them and engaging in a much larger and more computationally expensive experiment.

The CAPOW model assumes a level of capacity needed to meet demands of the 2016 grid, with future capacity additions limited to wind, solar, and battery storage. However, additions in renewable energy and battery capacity specified by the ReEDS scenarios take into account long-term increases in demand due to population growth. Thus, in order to separate the role of altered technology mix from any confounding effects related to population growth over the period 2020–2050, each ReEDS scenario's renewable energy capacity additions were first adjusted to 2016 load levels as follows:

$$\text{CAPOW capacity} = \left(\frac{\text{ReEDS capacity}}{\text{ReEDS average load}}\right) \times (\text{Historical Load}) \quad (1)$$

where

CAPOW capacity = installed capacity of wind/solar/battery storage in CAPOW (MW)
ReEDS capacity = installed capacity of wind/solar/battery storage in ReEDS scenario (MW)
ReEDS average load = average annual load in ReEDS scenario (MW)
Historical Load = average annual load over a 1000-year synthetic weather ensemble used in CAPOW model for 2016 grid (MW)

Our scenarios thus mimic ReEDS scenarios in terms of the individual ratios of installed wind, solar, and battery power capacity to average annual load. We then scale state level projections down to the balancing authority level.

We ignore future plant retirements, so any thermal power plant online today is essentially assumed to be available in 2050. This assumption was made primarily to avoid introducing differences in reserve margins (system reliability) across scenarios. It is important to note that the decision not to retire fossil fuel plants in the model does not necessarily equate to higher emissions; this capacity is simply left as extensive "back-up" capacity in the model. Due to variable renewable energy having a marginal cost of $0/MWh in the objective function, it is always taken first when available. This assumption does limit our ability to discuss simulation results in terms of commonly used reliability metrics (e.g., loss of load probability), since under most pathways our modeled systems have excess capacity. However, we do report alternative reliability metrics that may be valuable to system planners, such as the amount of dispatchable natural gas generation needed to avoid loss of load.

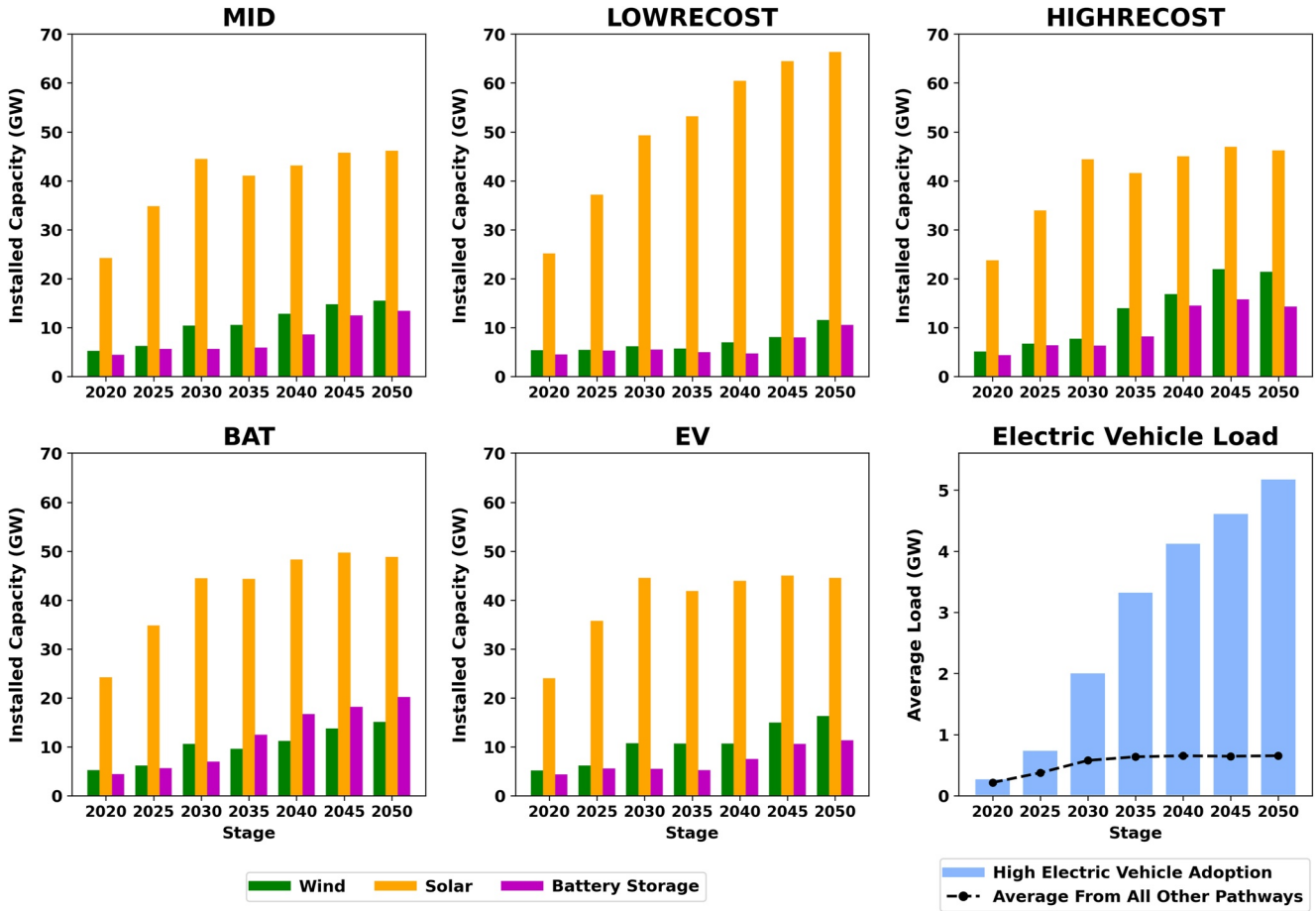

Figure 2. Renewable energy additions over time for each technology pathway in the California Independent System Operator (CAISO) system. Additions of wind, solar, and battery storage for each pathway are shown in five of the panels, while the sixth shows the average additional load experienced by the system due to electric vehicle adoption. In this bottom right panel, only the high electric vehicle adoption pathway is significantly different from the others.

Figure 2 shows capacity additions of clean technologies under each scenario for the CAISO system. A similar figure for the Mid-C market can be found in the Supporting Information S1 (Figure S1), while Figures S2 and S3 in the Supporting Information S1 show total capacity mixes over time for the CAISO and Mid-C systems, respectively. The main difference between these two systems is reliance on hydropower: in 2019, hydropower accounted for 16.8% of total electricity generation in CAISO and 62.4% of total electricity generation in the Mid-C market (United States Environmental Protection Agency, 2021). Additionally, the Mid-C system is not expected to add significant solar power due to its latitude.

For this study, we updated the original version of CAPOW to include representations of battery storage and electric vehicles. Battery storage was added to the mixed integer linear program in the form of a new type of generator with a single aggregate capacity for each of the 4 modeled zones in CAISO and a single aggregate capacity for the Mid-C market. Operational constraints on the batteries link and control the state of charge, energy balance across time (including battery efficiency losses) (Jurkovic et al., 2017; Li et al., 2016; Mohsenian-Rad, 2016; Senjyu et al., 2007), and charging and discharging rates (assumed to be 20% and 80% of the battery's total capacity, respectively) (Li et al., 2016; Senjyu et al., 2007). Battery operations directly affect the larger system power balance constraint, with the battery's discharge added to supply and the battery's charge added to load.

Electric vehicles were exogenously defined (added loads are outside the control of the optimization). We combine projections of electric vehicles adoption rates with pre-specified charging profiles per vehicle to get aggregate electric vehicle load for each zone in CAPOW. Electric vehicle adoption rates were estimated using data available from NREL's 2018 Electrification Futures Study (Mai et al., 2018a), which gives electric vehicle projections to 2050 under both a business-as-usual reference case and a high adoption case (Mai et al., 2018b). The high electric

vehicle (EV) pathway utilizes this high adoption case, while the other four pathways use reference electric vehicle levels. For simplicity, we assumed that the proportion of total electric vehicles that each state adopted was equal to its proportion of the national population. We used state population projection data (University of Virginia, 2018) to calculate the number of electric vehicles adopted in each state through 2050 and scaled this result back to only include the balancing authorities included within CAPOW. Figure 2 (bottom right panel) shows the load added to the system due to the inclusion of electric vehicle adoption under the high electric vehicle adoption (EV) pathway.

An aggregate 24 hr load profile giving the amount of power (in kW/vehicle) demanded at each hour of the day was adapted from Markel et al. (2010) and can be found in the Supporting Information S1 (Figure S4). This profile was assumed to not vary seasonally or inter-annually, consistent with ReEDS which does not model seasonal load shifting of vehicle charging (Brown et al., 2019). Multiplying the hourly profile by the number of electric vehicles gives the additional load that must be met by the system. We calculated the ratio of electric vehicle load in each hour to the average annual load simulated by the ReEDS model for each technology pathway, and then adjusted electric vehicle load in CAPOW to the same ratio. Note that our approach does not include any representation of controlled charging or any two-way, dynamic interaction between the grid and the aggregate electric vehicle charging profile. Although the ReEDS model can utilize dynamic diurnal charging profiles for load adjustment, EVs within ReEDS do not provide any other grid services. If system operators are allowed to optimize charging load, diurnal as well as interannual variation in charging patterns may emerge, which could be included in future work.

2.3. Synthetic Weather Generation

Air temperatures, streamflow, wind speeds, and solar irradiance are the main drivers of uncertainty in the CAPOW model, causing fluctuations in electricity demand and the availability of wind, solar, and hydropower. However, available records of hydrometeorological data are generally not long enough to capture the full range of plausible, multivariate extremes.

This study makes use of the same 1000-year stationary synthetic data set of air temperatures, streamflow, wind speeds, and solar irradiance described in Su, Kern, Reed, et al. (2020), which has been shown to closely reproduce observed statistical properties in weather and streamflow variables while also covering a wider range of conditions and plausible extremes. This synthetic data set covers 17 meteorological observation stations in the NOAA GHCN database (Menne, Durre, Korzeniewski, et al., 2012; Menne, Durre, Vose, et al., 2012) (mostly airports in major cities as well as areas with large installments of wind power); 6 sites from the National Renewable Energy Laboratory (NREL) National Solar Radiation Database (NSRDB); and 108 streamflow gages throughout the Pacific Northwest (Bonneville Power Administration, 2020) and California (State of California, 2020).

In previous work, it was found that 1,000 years is an appropriately sized synthetic data set for capturing uncertainty and combinatorial extremes in streamflow and weather (Su, Kern, Reed, et al., 2020). However, running each member of this 1000-year stochastic ensemble through the UC/ED model for each of the 35 unique future scenarios would have been prohibitively expensive computationally. Instead, the 1000-year data set was sampled to create a smaller 100-year data set of synthetic weather to explore within each scenario. Each stage of each technology pathway is then subjected to an identical 100-year synthetic weather sample, so that any resulting differences in performance across scenarios are due only to differences in the underlying technology mix.

Although the full 1000-year data set is reasonably representative of hydrometeorological uncertainty across the study domain, randomly sampling a small portion of this distribution would likely fail to capture the widest range of possible conditions. Therefore, we use a non-random sampling technique to expose the model to a more diverse set of conditions across variables. First, we select years with minimum, maximum, and 5th/95th percentiles in annual air temperatures, streamflow, wind speeds, and solar irradiance for both California and the Pacific Northwest (32 years). After these extreme years are chosen, the remaining years in the data set are filled out via a Latin hypercube sampling of the remaining 968 years based on annual statistics in order to achieve a more diverse combination of weather states, which may not reveal themselves in similarly sized random samples due to covariance (see Figure S5 in the Supporting Information S1).

Due to our non-random sampling approach, our results should not be viewed in terms of "risk" and/or the joint probability space of the hydrometeorological variables considered. Rather, our study provides a rigorous

Table 1
Ranges of Average CO_2 Reductions Experienced by 100 Weather Years From 2025 to 2050

Pathway	CAISO	Mid-C
MID	16.2%–39.4%	(−17.1%)–36.2%
LOWERCOST	14.8%–34.4%	8.0%–57.1%
HIGHERCOST	17.0%–50.6%	(−20.5%)–18.9%
EV	(−9.9%)−14.6%	(−21.0%)–17.2%
BAT	15.9%–41.5%	(−17.2%)–35.6%

Note. Reductions are given relative to 2020 and represent the percent change in average CO_2 emissions across weather years.

sensitivity analysis aimed at assessing possible vulnerabilities of the infrastructure system under a wider range of future conditions.

2.4. UC/ED Time Series Inputs

Time series of synthetic wind speeds and solar irradiance are used as inputs in multivariate regressions trained on observed data, which generate synthetic records of daily wind power and solar power production at each zone in CAPOW. These are then downscaled to an hourly time step by conditionally resampling from the historical record. Peak daily electricity demand is similarly estimated using multivariate regressions of historical air temperatures and wind speeds and then downscaled to an hourly time step. Streamflow data are used to simulate daily availability of hydropower in each zone of CAPOW using a combination of hydrologic mass balance and parameterized statistical models of hydroelectric dams in several major river basins. Daily volumes of hydropower are then dispatched optimally on an hourly basis by the optimization process in each UC/ED. In reality, dam operators have some operational discretion in shifting hydropower day-to-day in order to meet demand, which introduces the possibility that our methods over-constrain the flexibility of dams within week. These time series inputs are the same across scenarios, and additional details about their development in CAPOW are available in the Supporting Information S1 and in Su, Kern, Denaro, et al. (2020).

2.5. Performance Metrics

We track the performance of each scenario in terms of system-wide production costs (in $US), zonal market prices ($/MWh), greenhouse gas emissions (tons), and the amount of additional "firm capacity" needed to avoid loss-of-load (in MW, calculated as the maximum amount of electricity produced by "slack" variables in model simulations). Pushing the 100-year synthetic weather data set and each of 35 future grid scenarios through the CAPOW model's UC/ED framework gives 3,500 one-year model runs, each of which is evaluated on a seasonal, daily, and hourly basis.

Table 1 gives the average CO_2 emissions reductions experienced in each technology pathway after being run through the CAPOW model. Note that these reductions differ from values reported by NREL for the ReEDS model, likely due to differences in assumed heat rates of fossil fuel power plants and our detailed representation of grid operations. Particularly for the West Coast, where existing policy is targeting nearer-term decarbonization, the values shown in Table 1 may be conservative, that is, our '2050' technology adoption scenarios could occur well before this system experiences '2050' stress from population growth or climate change.

3. Results and Discussion

3.1. Interannual Variability

3.1.1. Comparing Weather Years Within a Single Technology Pathway

Our analysis of the simulation results is organized by timescale, beginning with a discussion of inter-annual variability in system performance across the full 3,500 model realizations (simulated years). Results are then interpreted on increasingly more resolved timescales, from seasonal phenomena down to hourly events. In the remainder of the paper, we assume a naming convention for each model realization that combines the technology mix (MID, BAT, EV, LOWRECOST, HIGHRECOST), future stage (2020, 2025 … 2050), system of interest (CAISO or Mid-C), and an integer from 0 to 99, representing a particular synthetic weather year.

We begin by exploring illustrative results for a single technology pathway (BAT) for the CAISO system (Figure 3). Similar plots for every technology pathway and region can be seen in the Supporting Information S1 (Figures S6–S14). The leftmost panel of these plots shows a color bar ranking of the 100 synthetic weather years based on the annual wholesale price of electricity. Each column represents a single technology stage (2020, 2025 … 2050); each row represents a single weather year and its performance across multiple future technology stages. As a single weather year is passed across future technology stages, its ranking in terms of average electricity price

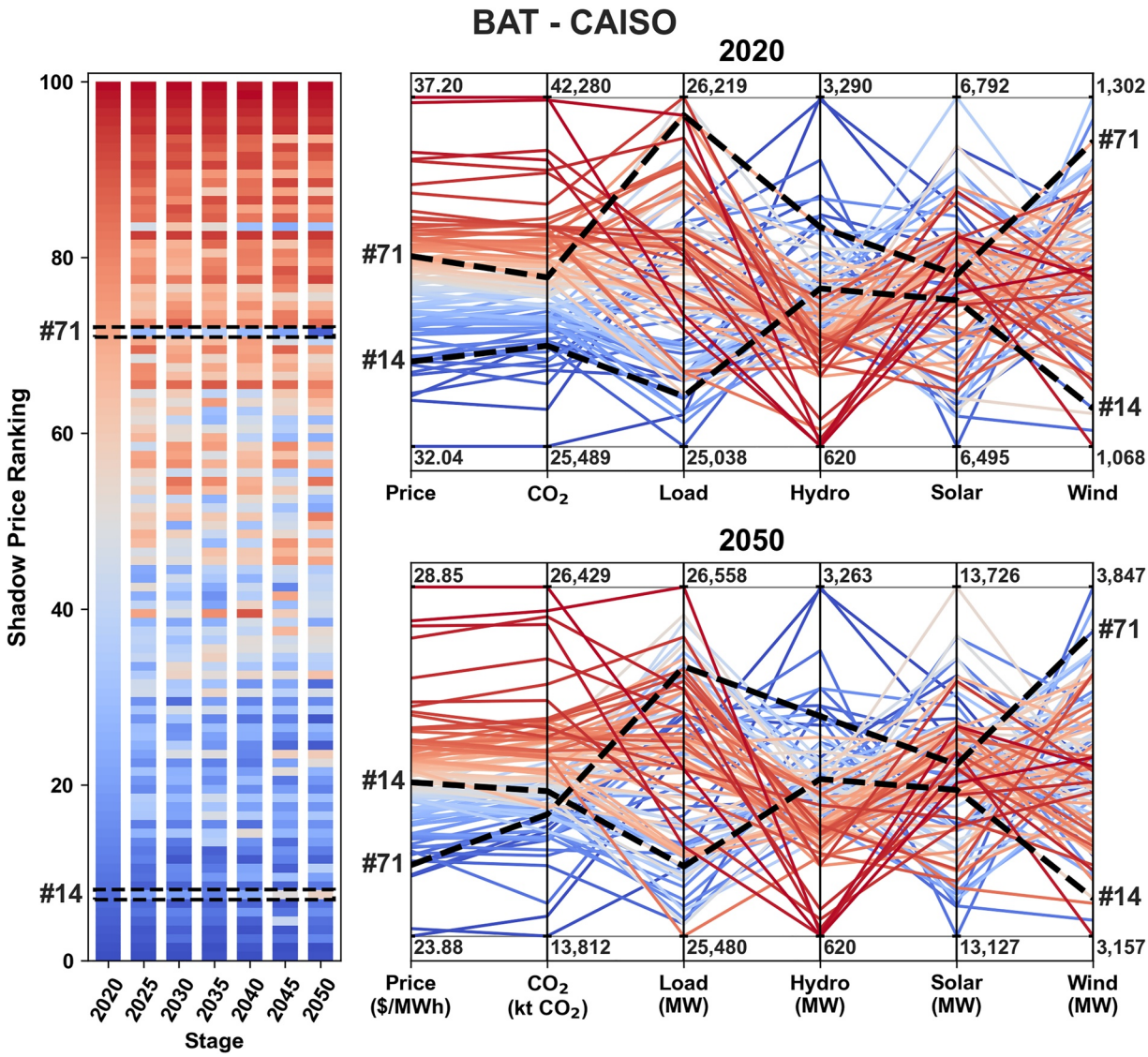

Figure 3. Price ranking distribution and parallel coordinates plots for BAT technology pathway in the CAISO system, with two weather years (#14 and #71) highlighted. The left panel shows a color bar ranking of the 100 synthetic weather years put through the model in terms of average annual wholesale electricity price; each row represents a single weather year and its performance across future technology stages. The right two panels show parallel coordinate plots of power system performance metrics and state variables over the 100 weather years for two future stages: 2020 (top) and 2050 (bottom). The color of each line corresponds to that year's price ranking (1–100) in that particular future stage, while its vertical position indicates its absolute value. Weather year #14 increases in price ranking from rank 8 to rank 57, due in part to very low wind power production, while weather year #71 decreases in price ranking from rank 72 to rank 5, due in part to very high wind power production.

(color) can change. For example, a row that gradually shifts from red to blue would signify a weather year that is a "high price" year in 2020 becoming a "low price" year in 2050, due to gradual evolution in the technology mix.

The panels on the right of Figure 3 (and in the Supporting Information S1 Figures S6–S14) are parallel coordinate plots of key power system performance metrics and state variables over the 100 weather years under two technology stages: 2020 (top) and 2050 (bottom). Each colored line represents a single model realization (year). The colors of each line correspond to its price ranking in that particular future stage, while the vertical position of each line along *y*-axes indicates absolute value. Minimum and maximum values of each column are shown to allow for comparison of absolute differences between 2020 and 2050.

Figure 3 shows an example of how individual weather years can switch from "good" to "bad" (and vice versa) across multiple stages of a single technology pathway. We highlight "BAT CAISO 14" and "BAT CAISO 71"

that is, weather years #14 and #71 in the CAISO system, under the low battery storage cost (BAT) technology pathway. Stacked generation plots for these simulation years are shown in Figure S15 in the Supporting Information S1, offering a finer scale, more mechanistic representation of what is happening within each of these two weather years.

In Figure 3, the price ranking columns at left indicate weather years #14 and #71 with black dashed boxes. The ranking of weather year #14 increases from rank 8 to rank 57 as it moves from 2020 to 2050 (color becomes progressively less blue and more red), while the ranking of weather year #71 decreases from rank 72 to rank 5, exhibiting the reverse trend. The reason for these differential shifts is explained in the parallel coordinate plots at right and stacked generation plots in the Supporting Information S1 Figure S15.

Weather year #71 is associated with higher load (this is caused by elevated late summer temperatures [see Figure S15 in the Supporting Information S1]); in 2020, this results in high prices. But, weather year #71 also experiences high levels of wind power production. As the BAT pathway in CAISO triples installed wind capacity from 2020 to 2050, increased wind power production works together with abundant hydropower during spring months to push fossil fuel generation out of the market and lower prices, while also helping to meet higher summer load (Figure S15 in the Supporting Information S1). On the other hand, weather year #14 is associated with one of the lowest annual wind power production values among the 100 synthetic weather years tested; as wind power becomes a larger segment of the generation mix, weather years #71 and #14 essentially switch places in rank order. Figures S23 and S24 in the Supporting Information S1 give another visualization of the magnitude of these re-rankings across scenarios.

3.1.2. Comparing a Single Weather Year Across Technology Pathways

Figure 4 shows a similar set of illustrative results that explore how increasing solar capacity can affect price sensitivity to irradiance. Here, we track a single weather year (#6, a year with low irradiance and available solar power production) under two different technology pathways in the CAISO system. Stacked generation plots for these simulation years are shown in the Supporting Information S1 (Figure S20). The two technology pathways shown, HIGHRECOST (the highest wind capacity pathway) and LOWRECOST (the highest solar capacity pathway), have very similar price rankings in 2020. However, the price ranking for weather year #6 under the HIGHRECOST pathway becomes steadily higher from 2020 to 2050 (increasing from rank 29 to rank 61), while its ranking under the LOWRECOST pathway increases through 2035, then declines, ending with roughly the same price rank in 2050 (rank 34) as in 2020 (rank 25). This result is, at first, somewhat confounding—why wouldn't a year with low irradiance become progressively 'worse' (more highly ranked) under a pathway that adds the most solar capacity?

There are two reasons for this. First, renewable energy curtailment due to excessive amounts of solar capacity may dampen the sensitivity of the market to interannual fluctuations in irradiance. Across every technology pathway explored, curtailment of solar generation in the CAISO market increases as more solar capacity is added. In the most extreme case (LOWRECOST), curtailment during spring months reaches >350GWh per day in 2050 (see Figure S21 in the Supporting Information S1). The degree of market oversaturation means that, even in a weather year with relatively low irradiance, there is still so much solar being produced that the market cannot absorb it all. In addition to curtailment, solar irradiance exhibits relatively low inter-annual variability, especially compared to wind speeds and streamflow. Differences in sensitivities of the CAPOW model's performance to variability in wind and solar are further explored in the following section.

3.1.3. Variance Decomposition and Tail Dependence

Figure 5 further explores the potential for weather year re-ranking to occur in the CAISO system across technology pathways. The top row of panels in Figure 5 show a variance decomposition of annual electricity price according to Sobol first order sensitivity indices across all 100 weather years for the MID, LOWRECOST, and HIGHRECOST technology pathways. Variance decomposition is used to separate and estimate the relative impact that individual variables as well as their interactive effects have on the total variance of a model output. This analysis was performed using the SALib package in Python.

The top panels in Figure 5 show the sensitivity to hydropower, load, solar power, wind power, and their interactive effects as a stacked bar plot for each future stage, with the size of each bar measuring the fraction of total variance in market prices explained by each variable. In other words, these bar plots illustrate the relative influence these

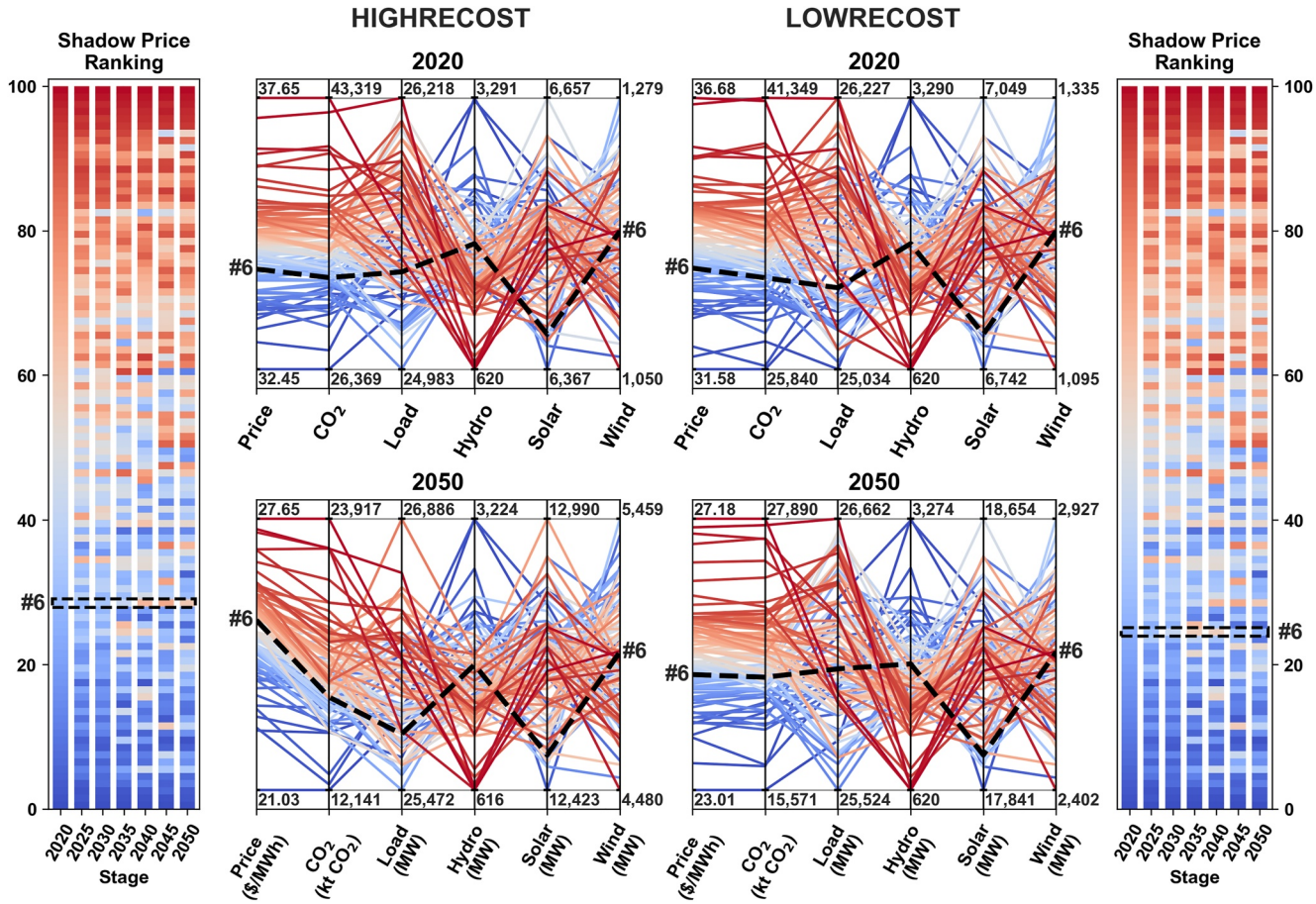

Figure 4. Comparison of HIGHRECOST and LOWRECOST pathways for weather year #6 in the California Independent System Operator system. Both technology pathways have very similar price rankings in 2020. However, the price ranking for weather year #6 under the HIGHRECOST pathway becomes steadily higher from 2020 to 2050 (increasing from rank 29 to rank 61), while its ranking under the LOWRECOST pathway increases through 2035, then declines, ending with roughly the same price rank in 2050 (rank 34) as in 2020 (rank 25).

four variables and their interactive effects have in controlling inter-annual fluctuations in market prices. The bottom panels in Figure 5 plot the upper and lower tail dependence coefficients between the rank of annual electricity price and the reverse rank of hydropower production across each future stage at thresholds of 0.9 and 0.1 (Rank 90 and Rank 10), respectively. Also shown in gray are similarly calculated dependence coefficients for the inner quintiles between 0.1 and 0.9. The tail dependence coefficient for the upper and lower tails is computed as the conditional probability that one rank in a bivariate distribution lies beyond the "tail" threshold, given that the other rank does. Therefore, these coefficients are measures of statistical dependence in the tails of the bivariate distribution between electricity price and hydropower availability in a given scenario. The inner quintile dependence coefficients divide the remaining 80% of the distribution into equal partitions (corresponding to bounded thresholds of 0.1–0.3, 0.3–0.5, 0.5–0.7, and 0.7–0.9), and represent the statistical dependence between price and hydropower within each partition. The coefficients for the inner quintiles measure the conditional probability that one rank lies within the given range, given that the other rank does. A tail dependence coefficient that is higher than the inner quintile dependence coefficients signifies a stronger influence on market prices from extreme hydrologic years than for more moderate years, and is seen in all three panels in the bottom row of Figure 5. Similar plots for the EV and BAT technology pathways, as well as for each scenario in the Mid-C market in the Pacific Northwest can be found in the Supporting Information S1 (Figures S25–S27).

The top row of panels in Figure 5 (as well as analogous Figures S25–S27 in the Supporting Information S1) confirm the dominant influence of inter-annual variability in hydropower in the sensitivity (variance) of market prices, followed by the interactive effects among the variables in the analysis. In CAISO, we found that solar power has the smallest effect on price sensitivity regardless of its relative installed capacity, due to a combination

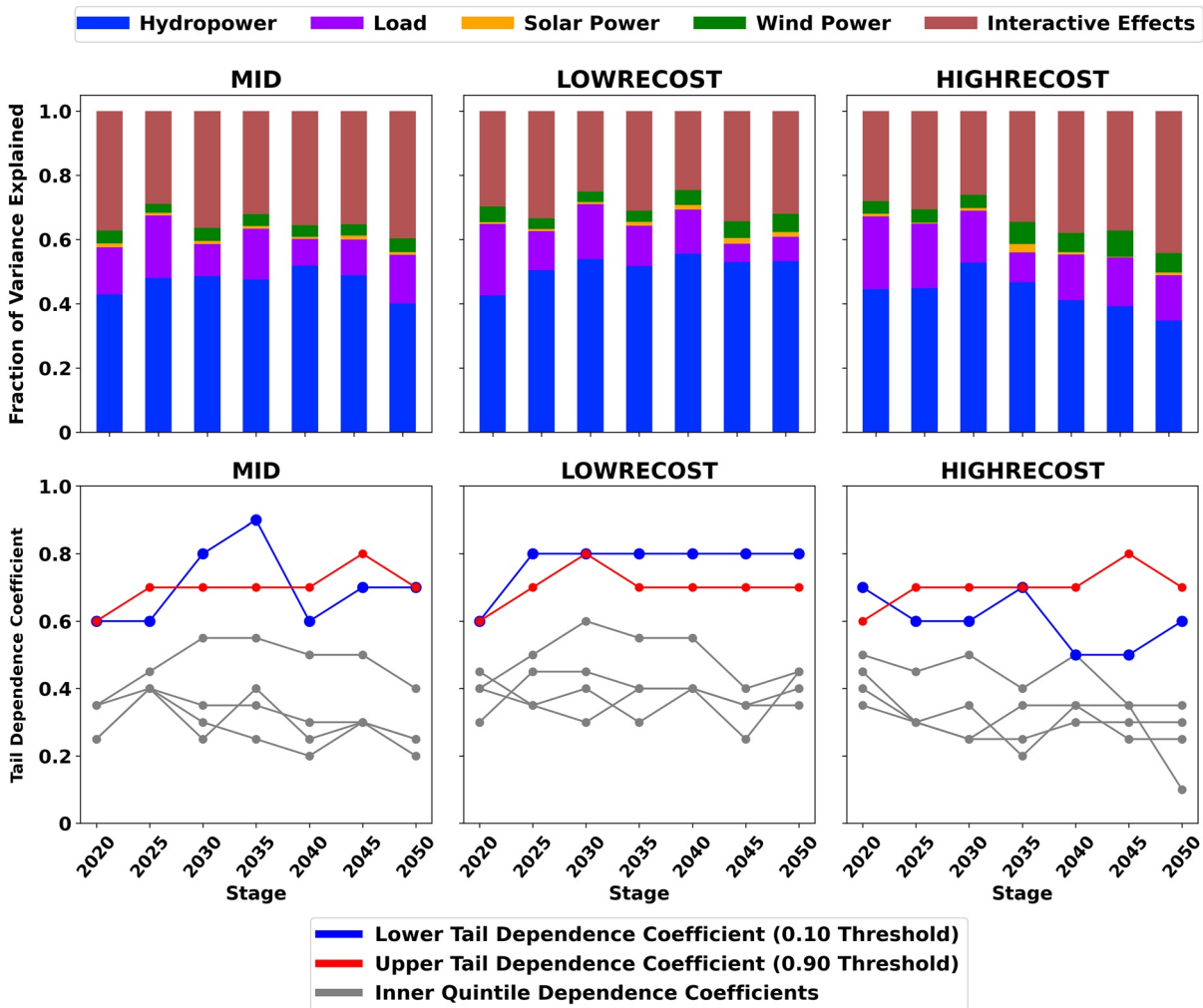

Figure 5. (top) Variance decomposition of annual electricity price across 100 weather years for three technology pathways in the California Independent System Operator system system, performed using the SALib library in Python; (bottom) Upper/lower tail dependence coefficients and inner quintile dependence coefficients between the rank of annual electricity price and reverse rank of hydropower production across each future stage for three technology pathways. Extreme price years remain firmly tied to hydrology (and to a lesser extent, temperature), while more moderate years result in more re-ranking. The upper tail dependence coefficient (correlation between very high price years and very low hydropower) tends to be even higher than the lower tail dependence coefficient. Plots for BAT and EV pathways and for pathways in the Mid-C system are given in Figures S25–S27 in the Supporting Information S1.

of lower inter-annual variability in solar irradiance and curtailment issues. Wind power, even with a much smaller share of the capacity mix, is responsible for a larger proportion of price sensitivity than solar power.

In general, we find that compared to CAISO, in the Mid-C market there is much less potential for weather year price rankings to shift across future stages and/or across technology pathways. The Mid-C system remains dominated by hydropower (or the lack thereof) into the future, and its price dynamics therefore remain more firmly tied to inter-annual fluctuations in streamflow.

Although there appears to be greater potential for re-ranking among weather years in the CAISO system, we nonetheless find that even there, the very highest and lowest ranked price years persistently map to extreme values in hydropower (a function of annual streamflow) and load (driven by summer air temperatures and cooling needs). For example, in Figures 3 and 4 we see that the bottom of each price ranking column is persistently deep blue (and the top is persistently red) across each column (stage), regardless of technology pathway considered. In the parallel coordinate plots, the highest price (red) years are associated with high load (caused mostly by hot summers) and low hydropower production, with the lowest price (blue) years experiencing the opposite. In both CAISO and the Mid-C system (Figures S10–S14 in the Supporting Information S1), five of the six highest-price

years in each system across all five technology pathways are the same weather years, for both 2020 and 2050. These five weather years also rank as the five lowest in hydropower production. In Figure 5, we found that the upper tail dependence coefficient was consistently higher than the lower, meaning that the relationship between very dry years and high prices is even stronger than the relationship between very wet years and low prices. This controlling influence of water scarcity does not change in later stages. Additionally, both tended to be higher than all of the inner quintile dependence coefficients, further suggesting the more persistent vulnerability in market prices to extreme hydrologic years.

Thus, despite the potential for future technology pathways to re-rank the importance of different weather years, the *most extreme years* in both the Mid-C system and CAISO are likely to remain firmly tied to hydrologic conditions, a finding with strong implications for the selection of "critical years" in reliability studies (Voisin et al., 2016). Even under pathways in which installed wind and solar increase by as much as 4x, variability in wind and solar power production across weather years is lower than it is for hydropower and load in the CAISO system. For the Mid-C system, the variability in hydropower is greater still (by a factor of about 3.5), though in this system the variability in available wind power is greater than that of load.

3.1.4. Distribution of Annual Electricity Prices

In Figure 6, we show the evolution and gradual dispersion of outcomes across technology pathways, in terms of distributions of annual electricity prices (left panel) and coefficient of variation (right panel). Note that all uncertainty shown in price distributions is due to variability across weather years. Figure S28 in the Supporting Information S1 shows similar information in terms of CO_2 emissions. In CAISO (top panels), market prices initially trend downward across all five pathways, and continue to decrease in each case except for the high electric vehicle adoption (EV) pathway. The EV adoption pathway in CAISO significantly increases in electric vehicle adoption around 2035, which is when we see average electricity prices begin to rise again due to significant added load to the system. The lowest prices in later years are achieved by the HIGHRECOST (highest wind) pathway, followed closely by the LOWRECOST (highest solar) pathway. The coefficient of variation is greatest for the HIGHRECOST pathway, suggesting that wind-heavy technology pathways could be most sensitive to inter-annual variability in prices due to weather.

For the Mid-C market in the Pacific Northwest, prices initially increase for four of the pathways, but eventually all decrease over time below 2020 levels, even for the EV pathway. The lowest prices here are in the LOWRECOST (highest wind and solar) pathway, with the highest prices in the HIGHRECOST (lowest wind and solar) pathway. Prices for the EV pathway do not increase as drastically as in CAISO, likely due to lower population and therefore fewer electric vehicles loading the system.

Note that the coefficient of variation is roughly an order of magnitude greater for the Mid-C system than for CAISO, due to significantly higher inter-annual variability in available hydropower (streamflow). The coefficient of variation also generally increases over time for all technology pathways. The technology pathways with the highest coefficients of variation in each system are the pathways with the most installed wind capacity in 2050 (LOWRECOST for the CAISO system and HIGHRECOST for the Mid-C system). This again suggests that, relative to solar power, increased dependence on wind power causes greater weather-based sensitivity in market prices. This effect is observed more strongly in CAISO, where hydropower has a less dominating influence.

3.2. Seasonality

Next, we move to a sub-annual timescale to extract insights not visible through averaged annual data. Figure 7 shows seasonality in 24-hr rolling average market prices in the CAISO system for three future stages. The darker lines in each panel along the bottom, middle, and top of the shaded region correspond to the minimum, median, and maximum average prices across the 100 weather years, respectively. The solid black lines in the 2035 and 2050 columns correspond to the median average price from 2020 for that technology pathway. A similar figure for the Mid-C market is shown in Figure S29 in the Supporting Information S1. Across all pathways, spikes in electricity prices are mainly concentrated in late summer and late winter, with the most drastic spikes seen in the EV technology pathway due to physical shortfalls or "loss-of-load" events. When CAPOW's modeled power system lacks sufficient generating capacity to meet demand for electricity and reserves in a given hour, a high-cost slack variable is triggered to meet the excess load. This represents a system shortfall, and designated shortfall hours are assigned a maximum market price of $1,000/MWh.

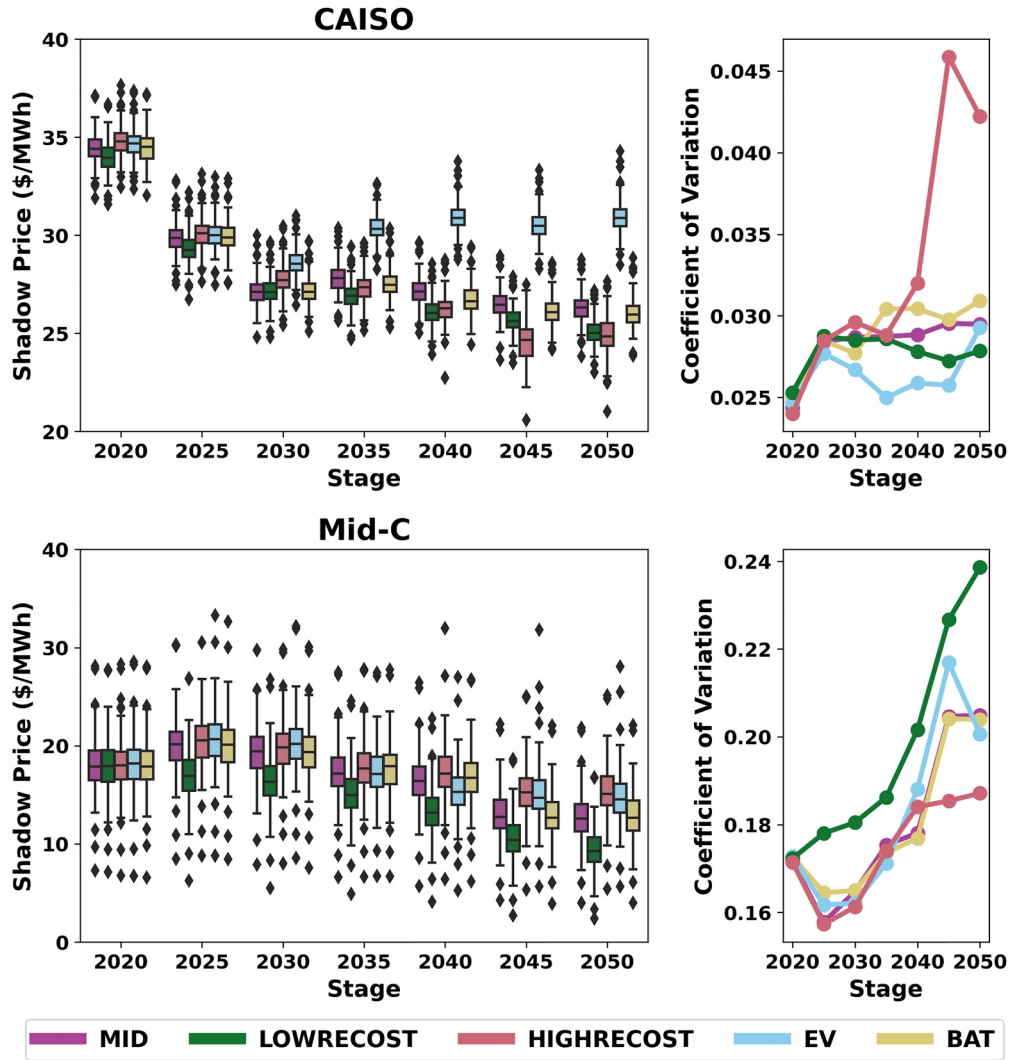

Figure 6. Boxplots of annual electricity price with coefficient of variation for all technology pathways for the California Independent System Operator (CAISO) (top) and Mid-C (bottom) systems. In the CAISO system, prices generally fall over time for each technology pathway except for the EV pathway. In the Mid-C system, four of the five pathways show initial increases in price, but all pathways fall below 2020 levels further into the future. The coefficient of variation in the right column is roughly an order of magnitude higher in the Mid-C than in CAISO, due mostly to significantly higher interannual variability in hydropower.

In general, the intra-annual dynamics of electricity prices remain most strongly influenced by seasonality in streamflow and temperatures, even as the grid evolves. However, certain technology pathways interact with this seasonal structure to dramatically lower prices or make them higher. In the case of the EV technology pathway, for example, added load from electric vehicles has the most severe impacts on market prices during late summer, when air temperatures (cooling demands) are high and streamflow (hydropower availability) is at an annual minimum. On the other hand, the lowest prices occur in the HIGHRECOST (highest wind) technology pathway during spring months, when abundant hydropower and wind power availability can cause the market to operate at near-zero electricity prices for extended periods. These depressed market prices are accompanied by high levels of curtailment (see Figure S22 in the Supporting Information S1). This effect can be seen to a lesser extent in the MID and BAT technology pathways.

Across most technology pathways, the range of possible prices in the CAISO system tightens from 2020 to 2035, then in 2050 becomes wider due to oversupply issues caused by excess renewables and periods of scarcity marked by more frequent price spikes. Thus, while added clean technology capacity does not influence the ranking of the

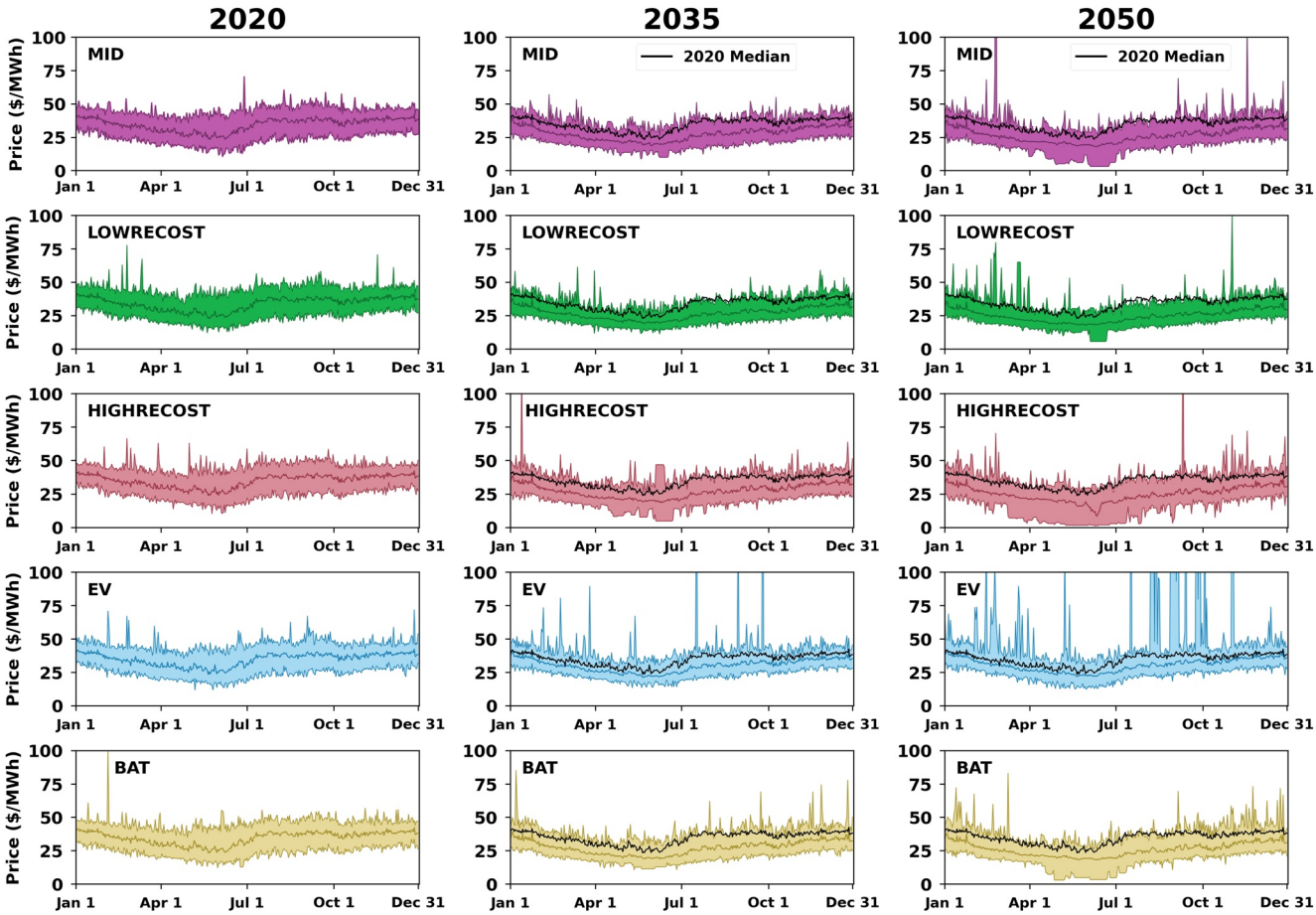

Figure 7. Daily rolling average electricity prices for the California Independent System Operator. System for each technology pathway in three future stages. The darker lines in each panel along the bottom, middle, and top of the shaded region correspond to the minimum, median, and maximum average prices across the 100 weather years, respectively. The solid black lines in the 2035 and 2050 columns correspond to the median average price from 2020 for that technology pathway. The left column shows very similar time series across technology pathways in 2020, while the middle and right columns show distinct variation across scenarios as well as across future stages.

most extreme weather years, it is clear that the evolving grid can create new, volatile price patterns as it interacts with hydrometeorological conditions on sub-annual timescales.

3.3. Hourly Impacts

Diurnal patterns of CAISO market prices for each season throughout the year can be seen in Figure S30 in the Supporting Information S1. In general, these appear deeply affected by the so-called 'duck curve', in which sub-daily price patterns are dominated by a trough of low prices during daylight hours, although there are notable differences across pathways. In particular, the EV scenario shows large increases of late afternoon/early evening load, and a dramatic need for ramping capacity along the "neck of the duck", when solar power production declines just as EV load is increasing. This phenomenon may pose specific risks for system reliability, and in fact the EV technology pathway in California contains an order of magnitude more supply shortfalls compared to the MID pathway, due primarily to the added load stressing the system as shown in Figure 2. Across all technology pathways in CAISO, the number of model years in which any loss-of-load (shortfall) event occurs in CAISO is greater for the EV pathway (163 years out of 700 (7 stages x 100 weather years)) than for all other pathways combined (113 years out of 2800 (4 pathways x stages x 100 weather years)). These events occur more often in later future stages, when the added load due to electric vehicle charging is greatest. In the Mid-C system, this same comparison is 35 in the EV pathway versus 13 in all other pathways combined. This observed increase in the system's susceptibility to failure is expected in our study, as any system experiencing a significant increase in

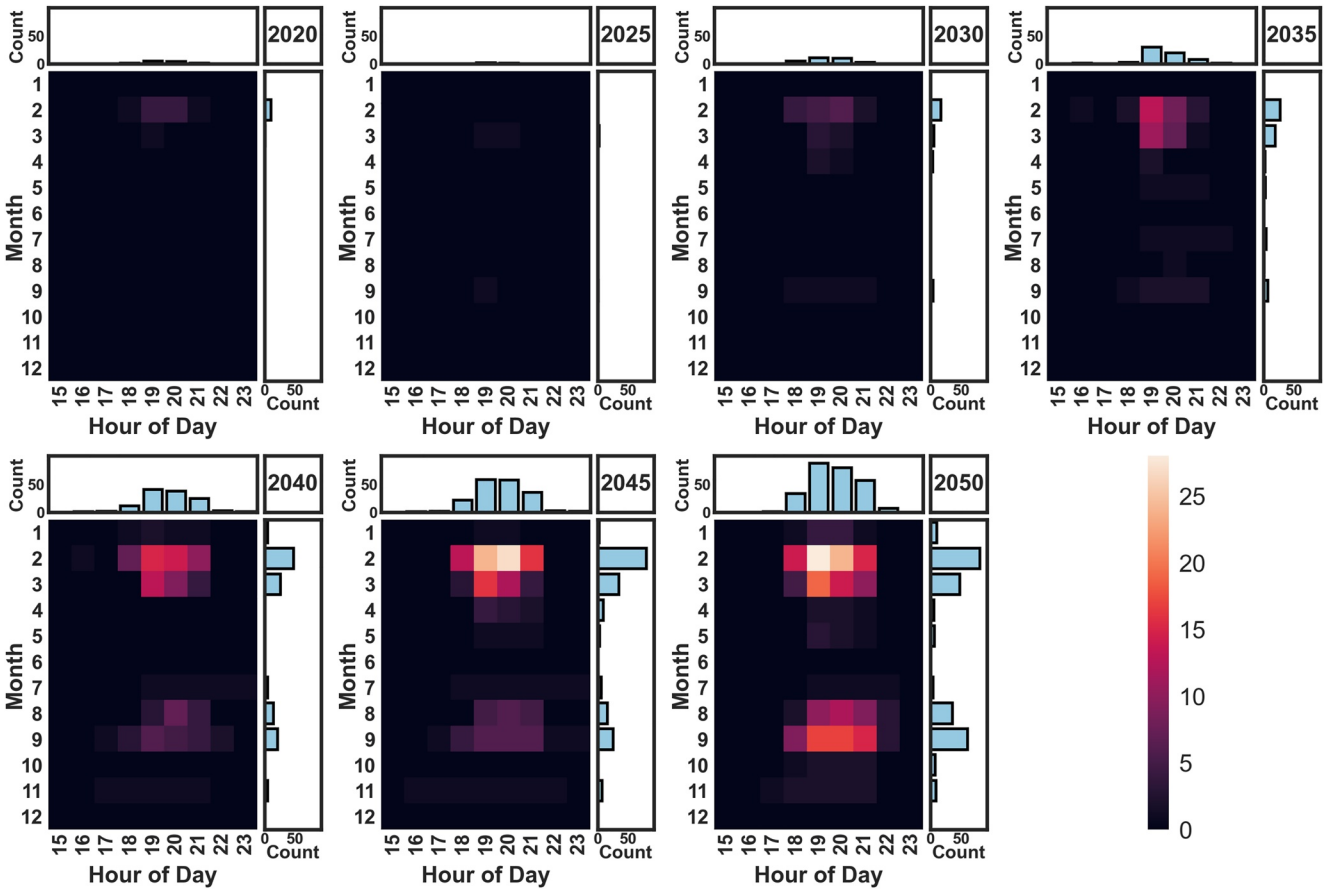

Figure 8. Heat maps showing shortfalls on two timescales in the California Independent System Operator system for EV technology pathway. Vertical axes show months of the year, while horizontal axes show evening hours of the day. Although the late winter shortfall events appear more frequently than in late summer, the severity of summer shortfalls was found to be much greater in terms of the total amount of slack generation dispatched.

static, inflexible load over time without any new generating capacity is likely pre-destined to fail. However, there is value in understanding how different hydrometeorological phenomena interact with added load dynamics from electric vehicle adoption to create system failures. For example, higher temperatures which stress the system with even more load during times of day with high vehicle charging and little or no available solar power could result in the system being unable to meet demand.

Figure 8 shows the frequency of system shortfalls under the EV technology pathway in California as heat maps on two timescales (month and hour-of-day). Only evening hours are shown in the plots, as earlier hours of the day contain virtually no shortfalls. We found that shortfalls (hours in which the high-cost slack variable is triggered) are concentrated in the late evening hours (consistent with the duck curve phenomenon) and are most frequent in late winter before the seasonal snowmelt, and in late summer months, after seasonal snowmelt when very little hydropower is available and air temperatures (cooling demands) remain high. Although the late winter shortfalls appear more frequently than in late summer, the severity of summer shortfalls is much greater in terms of the total amount of slack generation dispatched to meet demand (The total amount of slack generation dispatched in 2050 in CAISO for the EV technology pathway is 172 GWh in August-September, and 111 GWh in February-March). The absence of shortfalls in the middle months of the year confirms the important role of hydropower generated in California and imported from the Pacific Northwest during the annual snowmelt. A similar figure for the Mid-C system is given in Figure S31 in the Supporting Information S1. In general, the Mid-C system is also susceptible to shortfalls in the late summer months, as well as throughout the winter when temperatures are low. There are fewer shortfalls in the Mid-C system, however, with many of the shortfall events occurring during a single stretch of several hours during one year.

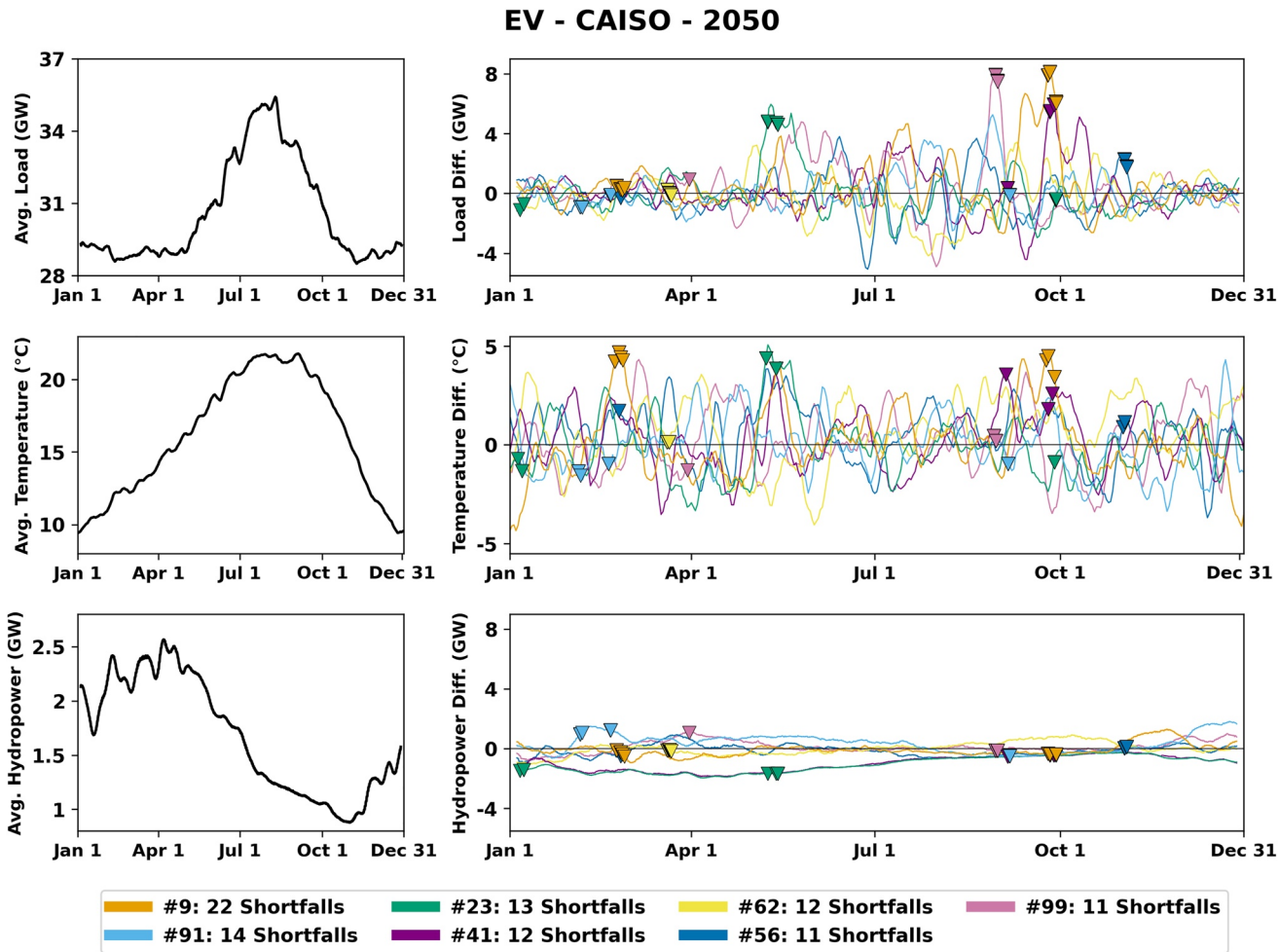

Figure 9. Time series of anomalies in power system for EV technology pathway in the California Independent System Operator system in 2050, with shortfalls. The left column shows a weekly rolling average time series across all 100 weather years, while the right column shows anomalies relative to these weekly rolling average values for seven chosen weather years, with the timing of individual shortfall events marked with triangles in each plot. Many of the shortfall events are associated with high positive temperature anomalies, which cause drastic spikes in load.

The shortfalls shown in Figure 8 are aggregated from all 100 synthetic weather years run through the model for the CAISO system under the EV technology pathway. However, the appearance of shortfalls is not evenly distributed among all years. The underlying hydrometeorological conditions of a given year and their combined effects on very short timescales contribute to the timing and magnitude of shortfall events. Figure 9 shows the occurrence of supply shortfalls under the EV technology pathway in 2050 in the CAISO system. The seven weather years shown are responsible for more than 33% of the total number of shortfall events across all 100 weather years in this scenario. The left column of the figure shows the weekly rolling average values of load, temperature, and hydropower across all 100 weather years in the EV technology pathway. The right column of the figure shows anomalies relative to these weekly rolling average values for the seven chosen weather years, with the timing of shortfalls marked with triangles in each plot. More detailed portraits of each of the seven chosen weather years are shown in Figures S32 and S33 in the Supporting Information S1. Also available the Supporting Information S1 is a similar series of plots for the Mid-C system (Figures S34–S36).

We find that shortfalls in CAISO under the EV 2050 scenario often occur during periods of high positive temperature anomalies; in late spring and summer, these heat waves usually translate to very large temporary increases in electricity demand. Two of the weather years shown (#23 and #41) are extreme drought years. However, drought-caused deficits in hydropower are most severe during the snowmelt period and have less of a connection to late summer reliability failures. While we do see some supply shortfalls caused by an extreme hydropower

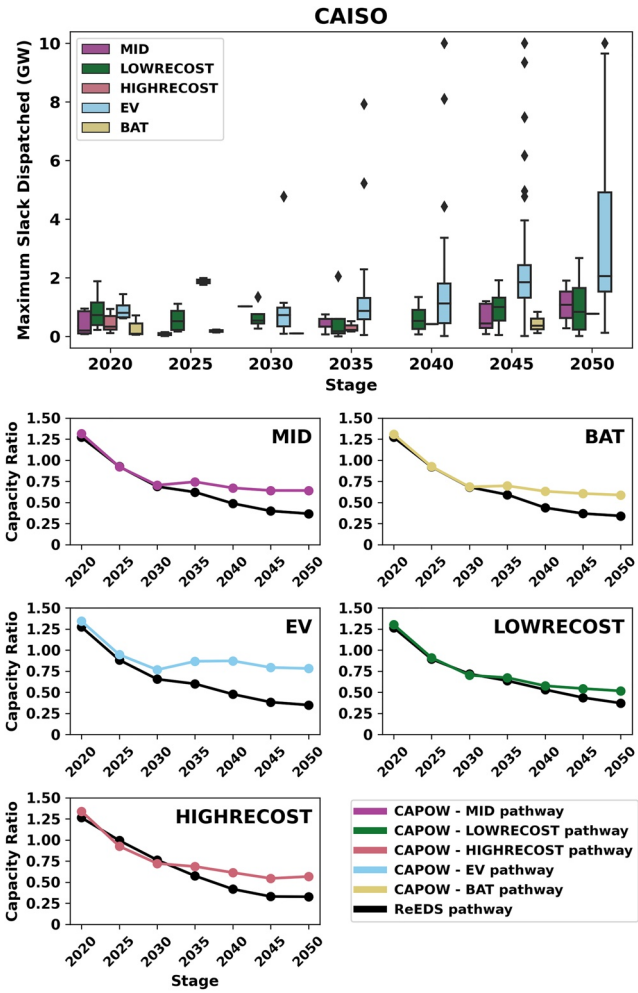

Figure 10. (top) Boxplots showing distribution of maximum slack generation dispatched in the California Independent System Operator (bottom) Ratio of thermal dis-patchable capacity plus the maximum amount of slack dispatched to total wind and solar power capacity for each scenario in the CAISO system in CAPOW. Shown in black are the ratios of thermal dis-patchable capacity to total wind and solar capacity for each scenario in the ReEDS model. After around 2030, the ratios shown in the bottom half of the figure begin to separate distinctly.

deficit occurring during a heat wave (e.g., weather year #23 in May), negative hydropower anomalies during supply shortfalls are typically quite small in an absolute sense, because late summer months are marked by extremely low hydropower availability even under normal circumstances. In contrast, Figures S34–S36 in the Supporting Information S1 show that for the Mid-C system, the effect of low hydropower anomalies seems to eclipse the effects of load and temperature in determining the system's susceptibility to shortfalls.

Several other shortfalls in late winter and early spring in Figure 9 occurred during periods of low wind and solar power anomalies as well, which can combine with even small negative hydropower anomalies to cause a shortfall. In reality, the lower severity of the late winter and early spring shortfalls could result in events that grid operators could handle without a failure.

3.4. Analysis of Capacity and Reliability Requirements

For each instance of the slack variable being triggered, we track the amount of load unable to be met by the system in that hour. In reality, demand response measures and various other tools are used to prevent blackouts in minor cases, but a severe shortage of generation capacity will cause a system failure. Recently, this occurred in California, when an extreme heat wave caused the system operator to trigger rolling blackouts in the summer of 2020 (Roth, 2020). The top panel of Figure 10 shows the distribution of maximum values recorded for the slack variable in any hour over the 100 weather years for each technology pathway and future stage. This value, which represents the largest deficit in generating capacity experienced by a given technology pathway in a given year, varies considerably across both pathways and future stages.

These values can be used as a first-order preliminary approximation of additional dispatchable generating capacity needed to achieve 100% reliability in the system. The bottom panels of Figure 10 show for each scenario the ratio of total thermal dispatchable capacity (plus the maximum slack value triggered to meet demand) to total wind and solar power capacity. This capacity ratio represents the amount of thermal dispatchable capacity required for every unit of wind and solar power capacity to ensure reliability in the system. Also shown in black in these plots is the same capacity ratio calculated for each scenario in the ReEDS model (slack values not included). Here, a lower ratio represents less dispatchable thermal capacity being required for each unit of wind and solar power capacity to ensure reliability. A similar figure for the Mid-C system is given in Figure S33 in the Supporting Information S1.

We find that in CAISO, the capacity needed in CAPOW to ensure reliability across the 100 synthetic weather years diverges from the ReEDS values in future technology stages, with the ratios in the CAPOW model becoming higher than ratios suggested by ReEDS for the same scenario. This suggests that when ReEDS scenarios are subjected to a 100-year weather sensitivity analysis, the amount of thermal dispatchable capacity given by ReEDS would lead to regular system failures in CAPOW. In the Mid-C system, however, we find the opposite (the required capacity ratio is generally lower in CAPOW than in ReEDS, suggesting that ReEDS may be overly conservative in assigning dispatchable capacity in that system). Overall, this finding points to the need for more robust representation of uncertainty and compound extremes in longer term capacity planning models.

4. Conclusion

In this study, we explore how different grid technology pathways could influence the vulnerability of the U.S. West Coast bulk power system to hydrometeorological uncertainty. We modeled the operations of the CAISO and Mid-C markets under five different technological pathways based on NREL ReEDS scenarios at five-year

intervals from 2020 to 2050. Each combination of technology pathway and future year was run through the CAPOW grid operations model using a 100-year synthetic weather data set, which was sampled from a larger 1000-year ensemble. We assume climate stationarity; in reality, decarbonization could occur while the system simultaneously experiences impacts from climate change (increased frequency and severity of heat waves, altered streamflow dynamics) and population growth (long term increases in demand). Future work in this area should explore the combinatorial effects and potential vulnerabilities of an evolving technology mix and nonstationary climate. Nonetheless, examining the effects of altered technology mix in isolation does allow for a number of advantages and insights that could be applicable to systems decarbonizing quickly. From a planning perspective, this study is representing a world in which the transition to renewable energy in the power sector occurs much faster (i.e., "overnight") along the West Coast. The reality probably lies somewhere between the gradual transitions explored in the NREL ReEDS scenarios and our representation of increased renewable energy adoption without considering concurrent increases in demand, altered hydroclimate, etc.

Our results show that in both the CAISO and Mid-C markets, shifts in the underlying grid technology mix cause weather years to "re-rank" in terms of average wholesale prices, that is, "good" years can become "bad" years, and vice versa. This ranking is a critical process for reliability and resource adequacy studies, as typically only a small number of critical weather years are considered. Re-ranking occurs when the underlying hydrometeorological conditions of a given year (e.g., average wind speeds, irradiance) become more/less advantageous as the grid changes. There appears to be considerably more potential for this phenomenon in the CAISO system compared to the Mid-C.

In general, we find that higher wind scenarios become more sensitive to interannual variability in wind speeds, and wind heavy technology scenarios show the greatest interannual variability in prices. In contrast, lower interannual variability in irradiance and the impacts of curtailment from overbuilding solar capacity appear to dampen sensitivity to interannual fluctuations in solar availability.

One of our most consistent findings across both systems and across all scenarios tested is that the very highest and lowest ranking years in terms of average electricity price remain firmly tied to extremes in hydropower availability (streamflow) and load (summer air temperatures). In both CAISO and the Mid-C markets, the highest-price years in 2020 are a group of years with extremely low hydropower production. The same weather years rank as the highest-price years in 2050. In particular, we find that low hydropower remains the most important influence in causing years of extreme (high) prices. Thus, even as the West Coast decarbonizes, drought will remain a key vulnerability.

We also find that the current seasonal dynamics in market prices on the West Coast, which are controlled primarily by spring snowmelt followed by hotter, dry weather in late summer and fall, remain largely intact out to 2050. In the CAISO system, the main concentrations of supply shortfalls tend to be late summer (the hottest and most dry part of the year) and late winter (just before the annual snowmelt adds significant hydropower to the system).

Supply shortfalls are most frequent under the high electric vehicle adoption pathway, in which a large amount of load is added to the system. This outcome was expected, as no new generating capacity was constructed to meet this added load, but using this pathway allowed us to examine the specific conditions leading to failure. In the CAISO system, shortfalls occurred almost entirely in the evening hours of the day, after the sun sets and while demand is still high. We also show that the occurrence of these failures is clustered in a smaller group of weather years. We found that high positive temperature anomalies were present for most shortfalls, suggesting that heat waves during late summer (when there is very little hydropower available even in 'normal' water years) are most responsible for system failures. In the Mid-C system, supply shortfalls are much more strongly tied to streamflow anomalies.

Finally, by analyzing the maximum amount of slack generation dispatched for each scenario, we found that the ratio of dispatchable thermal capacity to variable renewable energy capacity present in existing capacity expansion models like ReEDS may significantly underestimate the amount needed to ensure a reliable grid under stationary weather uncertainty. However, future work is needed to examine if these results apply equally across other existing capacity expansion models. In general, future work exploring hydrological uncertainty more deeply is needed to assess the ability of long-term planning models to provide capacity mixes which represent systems that are reliable.

Oversupply events, as a result of the simplified zonal transmission network in the CAPOW model, may have a biased representation. Within each modeled zone, there is no gradient of locational marginal price, which would be necessary to capture lower-level dynamics influenced by transmission constraints. In the case of oversupply of renewable energy, a more detailed transmission network could increase curtailment and reduce decarbonization.

The results of this study provide insights that could be applicable to power systems attempting to decarbonize in the face of deeply uncertain variability in weather. The persistent vulnerability of the US West Coast power system to droughts and heat waves as seen in the summers of 2020 and 2021 (Reyes-Velarde & Pinho, 2021; Smith, 2020) will continue to pose significant challenges for utilities, system planners, and regulatory bodies even as more variable renewable energy is added to the system. In fact, large amounts of wind and solar capacity may lead to significant levels of curtailment while still being unable to meet reliability requirements. In order to operate reliably, the current dependence on hydropower in this system may still require significant amounts of natural gas capacity to meet load during a drought. This backup capacity could make deep decarbonization not only more expensive, but also more difficult to achieve without innovation, and may be systematically underestimated in existing longer term planning models.

Data Availability Statement

The data that were used in this analysis can be found at: https://doi.org/10.5281/zenodo.5775067. The CAPOW model used in this study can be found at: https://doi.org/10.5281/zenodo.4720762.

Acknowledgments
This research was supported by the US Department of Energy, Office of Science, as part of research in the MultiSector Dynamics, Earth and Environmental System Modeling Program, as well as the National Science Foundation INFEWS program, award #1639268 (T2).

References

Bain, D., & Acker, T. (2018). Hydropower impacts on electrical system production costs in the southwest United States. *Energies*, *11*(2), 368. https://doi.org/10.3390/en11020368

Bonneville Power Administration. (2020). *Historical streamflow data*. Retrieved from https://www.bpa.gov/p/Power-Products/Historical-Streamflow-Data/Pages/Historical-Streamflow-Data.aspx

Brown, M., Cole, W., Eurek, K., Becker, J., Bielen, D., Chernyakhovskiy, I., et al. (2019). *Regional energy deployment system (ReEDS) model documentation: Version 2019*, National Renewable Energy Laboratory. (NREL). NREL/TP-6A20-74111. Retrieved from https://www.nrel.gov/docs/fy20osti/74111.pdf

Bruninx, K., & Delarue, E. (2017). *Improved energy storage system & unit commitment scheduling* (pp. 1–6). IEEE Manchester PowerTech. https://doi.org/10.1109/PTC.2017.7981000

Bushnell, J., & Novan, K. (2018). Setting with the sun: The impacts of renewable energy on wholesale power markets. *Econometric Modelling: Commodity Markets eJournal*. https://doi.org/10.3386/W24980

Clean Energy Technology Center. (2021). *Database of state incentives for renewables & efficiency (DSIRE)*. Retrieved from https://www.dsireusa.org

Cole, W., Gates, N., Mai, T., Greer, D., & Das, P. (2019). *Standard scenarios report: A U.S. Electricity sector outlook*. National Renewable Energy Laboratory. (NREL). NREL/TP-6A20-74110. Retrieved from https://www.nrel.gov/docs/fy20osti/74110.pdf

De Jonghe, C., Delarue, E., Belmans, R., & D'haeseleer, W. (2011). Determining optimal electricity technology mix with high level of wind power penetration. *Applied Energy*, *88*(6), 2231–2238. https://doi.org/10.1016/j.apenergy.2010.12.046

Denholm, P., Ela, E., Kirby, B., & Milligan, M. (2010). *The role of energy storage with renewable electricity generation*. National Renewable Energy Laboratory. (NREL). NREL/TP-6A2-47187. Retrieved from https://www.nrel.gov/docs/fy10osti/47187.pdf

Denholm, P., Margolis, R., & Milford, J. (2008). *Production cost modeling for high levels of photovoltaics penetration*. National Renewable Energy Laboratory. (NREL). NREL/TP-581-42305. https://doi.org/10.2172/924642

Denholm, P., Nunemaker, J., Gagnon, P., & Cole, W. (2019). The potential for battery energy storage to provide peaking capacity in the United States. *Renewable Energy*, *151*, 1269–1277. https://doi.org/10.1016/j.renene.2019.11.117

Energy and Environmental Economics Inc. (2014). *California transportation electrification assessment phase 2: Grid impacts*. Retrieved from https://www.caletc.com/wp-content/uploads/2016/08/CalETC_TEA_Phase_2_Final_10-23-14.pdf

Haas, J., Cebulla, F., Nowak, W., Rahmann, C., & Palma-Behnke, R. (2018). A multi-service approach for planning the optimal mix of energy storage technologies in a fully-renewable power supply. *Energy Conversion and Management*, *178*, 355–368. https://doi.org/10.1016/j.enconman.2018.09.087

Hadley, S. W., & Tsvetkova, A. (2009). Potential impacts of plug-in hybrid electric vehicles on regional power generation. *The Electricity Journal*, *22*(10), 56–68. https://doi.org/10.1016/j.tej.2009.10.011

Han, J., Park, J., & Lee, K. (2017). Optimal scheduling for electric vehicle charging under variable maximum charging power. *Energies*, *10*(7). https://doi.org/10.3390/en10070933

Johnson, J. X., De Kleine, R., & Keoleian, G. A. (2014). Assessment of energy storage for transmission-constrained wind. *Applied Energy*, *124*, 377–388. https://doi.org/10.1016/j.apenergy.2014.03.006

Jordehi, A. R. (2018). How to deal with uncertainties in electric power systems? A review. *Renewable and Sustainable Energy Reviews*, *96*, 145–155. https://doi.org/10.1016/j.rser.2018.07.056

Joskow, P. L. (2019). Challenges for wholesale electricity markets with intermittent renewable generation at scale: The U.S. Experience. *Oxford Review of Economic Policy*, *35*(2), 291–331. https://doi.org/10.1093/oxrep/grz001

Jurkovic, K., Pandzic, H., & Kuzle, I. (2017). *Robust unit commitment with large-scale battery storage*, IEEE Power & Energy Society General Meeting, (pp. 1–5) https://doi.org/10.1109/PESGM.2017.8274302

Kavalec, C., Gautam, A., Jaske, M., Marshall, L., Movassagh, N., & Vaid, R. (2018). *California energy demand 2018 — 2030 revised forecast*. California Energy Commission, Electricity Assessments Division, CEC-200-2018-002-CMF. Retrieved from https://efiling.energy.ca.gov/getdocument.aspx?tn=223244

Li, N., & Hedman, K. W. (2015). Economic assessment of energy storage in systems with high levels of renewable resources. *IEEE Transactions on Sustainable Energy*, *6*(3), 1103–1111. https://doi.org/10.1109/TSTE.2014.2329881

Li, N., Uckun, C., Constantinescu, E. M., Birge, J. R., Hedman, K. W., & Botterud, A. (2016). Flexible operation of batteries in power system scheduling with renewable energy. *IEEE Transactions on Sustainable Energy*, *7*(2), 685–696. https://doi.org/10.1109/TSTE.2015.2497470

Madani, K., & Lund, J. R. (2010). Estimated impacts of climate warming on California's high-elevation hydropower. *Climatic Change*, *102*(3), 521–538. https://doi.org/10.1007/s10584-009-9750-8

Mai, T., Jadun, P., Logan, J., McMillan, C., Muratori, M., Steinberg, D., et al. (2018a). *Electrification futures study: Scenarios of electric technology adoption and power consumption for the United States*. National Renewable Energy Laboratory. (NREL). NREL/TP-6A20-71500. Retrieved from https://www.nrel.gov/docs/fy18osti/71500.pdf

Mai, T., Jadun, P., Logan, J., McMillan, C., Muratori, M., Steinberg, D., et al. (2018b). Electrification Futures Study Demand-side Scenarios report figure data [Dataset]. National Renewable Energy Laboratory (NREL).https://doi.org/10.7799/1460948Pubmed Partial Author stitle stitle Volume Page

Mai, T., Wiser, R., Sandor, D., Brinkman, G., Heath, G., Denholm, P., et al. (2012). *Exploration of high-penetration renewable electricity futures, vol. 1 of renewable electricity futures study*. National Renewable Energy Laboratory. (NREL). NREL/TP-6A20-52409-1. https://doi.org/10.2172/1046880

Markel, T., Mai, T., & Kintner-Meyer, M. (2010). *Transportation electrification load development for a renewable future analysis: Preprint*. National Renewable Energy Laboratory. (NREL) NREL/CP-5400-49181. Retrieved from http://www.osti.gov/bridge

Menne, M. J., Durre, I., Korzeniewski, B., McNeal, S., Thomas, K., Yin, X., et al. (2012). Global historical climatology network-daily (GHCN-Daily), version 3 [Dataset]. NOAA National Climatic Data Center. https://doi.org/10.7289/V5D21VHZ

Menne, M. J., Durre, I., Vose, R. S., Gleason, B. E., & Houston, T. G. (2012). An overview of the global historical climatology network-daily database. *Journal of Atmospheric and Ocean Technology*, *29*(7), 897–910. https://doi.org/10.1175/JTECH-D-11-00103.1

Mohsenian-Rad, H. (2016). Optimal bidding, scheduling, and deployment of battery systems in California day-ahead energy market. *IEEE Transactions on Power System*, *31*(1), 442–453. https://doi.org/10.1109/TPWRS.2015.2394355

Nikolewski, R. (2019). *California electric vehicle sales are up. But will we reach the 5 million goal by 2030?*. Los Angeles Times. Retrieved from https://www.latimes.com/business/story/2019-12-01/electric-vehicle-sales-in-california-on-the-rise-but-is-it-enough-to-reach-the-5-million-goal-by-2030

Pereira, F. B., Paucar, V. L., & Saraiva, F. S. (2018). Power system unit commitment incorporating wind energy and battery energy storage. In. IEEE XXV international conference on electronics, electrical engineering and computing, (pp. 1–4). https://doi.org/10.1109/INTERCON.2018.8526431

Reyes-Velarde, A., & Pinho, F. E. (2021). *Blistering heat wave sets record temperatures across California*. Los Angeles Times. Retrieved from https://www.latimes.com/california/story/2021-07-11/record-breaking-temperatures-set-as-heat-wave-continues-across-california

Roth, S. (2020). *What caused California's rolling blackouts? Climate change and poor planning*. Los Angeles Times. Retrieved from https://www.latimes.com/environment/story/2020-10-06/california-rolling-blackouts-climate-change-poor-planning

Seel, J., Mills, A., & Wiser, R. (2018). *Impacts of high variable renewable energy futures on wholesale electricity prices, and on electric-sector decision making*. Lawrence Berkeley National Laboratory. (LBNL). LBNL-2001163, Retrieved from https://emp.lbl.gov/publications/impacts-high-variable-renewable

Senjyu, T., Miyagi, T., Yousuf, S. A., Urasaki, N., & Funabashi, T. (2007). A technique for unit commitment with energy storage system. *International Journal of Electrical Power Energy System*, *29*(1), 91–98. https://doi.org/10.1016/j.ijepes.2006.05.004

Smith, H. (2020). *Fall heat wave breaks records, prompts statewide flex alert to conserve energy*, Los Angeles Times. Retrieved from https://www.latimes.com/california/story/2020-10-01/fall-heat-wave-breaks-records-prompts-statewide-flex-alert-to-conserve-energy

Staffell, I., & Pfenninger, S. (2018). The increasing impact of weather on electricity supply and demand. *Energy*, *145*, 65–78. https://doi.org/10.1016/j.energy.2017.12.051

State of California. (2020). California Data Exchange Center. Retrieved from https://cdec.water.ca.gov/

Steinberg, D., Bielen, D., Eichman, J., Eurek, K., Logan, J., Mai, T., et al. (2017). *Electrification and decarbonization: Exploring U.S. Energy use and greenhouse gas emissions in scenarios with widespread electrification and power sector decarbonization*. National Renewable Energy Laboratory. (NREL). NREL/TP-6A20-68214. https://doi.org/10.2172/1372620

Su, Y., Kern, J. D., Denaro, S., Hill, J., Reed, P., Sun, Y., et al. (2020). An open source model for quantifying risks in bulk electric power systems from spatially and temporally correlated hydrometeorological processes. *Environmental Modelling & Software*, *126*, 104667. https://doi.org/10.1016/j.envsoft.2020.104667

Su, Y., Kern, J. D., Reed, P. M., & Characklis, G. W. (2020). Compound hydrometeorological extremes across multiple timescales drive volatility in California electricity market prices and emissions. *Applied Energy*, *276*, 115541. https://doi.org/10.1016/j.apenergy.2020.115541

Sun, M., Teng, F., Konstantelos, I., & Strbac, G. (2018). An objective-based scenario selection method for transmission network expansion planning with multivariate stochasticity in load and renewable energy sources. *Energy*, *145*, 871–885. https://doi.org/10.1016/j.energy.2017.12.154

Tarroja, B., Aghakouchak, A., & Samuelsen, S. (2016). Quantifying climate change impacts on hydropower generation and implications on electric grid greenhouse gas emissions and operation. *Energy*, *111*, 295–305. https://doi.org/10.1016/j.energy.2016.05.131

Trabish, H. K. (2017). *Prognosis negative: How California is dealing with below-zero power market prices*, Utility Dive. Retrieved from https://www.utilitydive.com/news/prognosis-negative-how-california-is-dealing-with-below-zero-power-market/442130/

United States Environmental Protection Agency. (2021). *Emissions & generation resource integrated database (eGRID), 2019*. Office of Atmospheric Programs. Retrieved from https://www.epa.gov/egrid

University of Virginia, Weldon Cooper Center, Demographics Research Group. (2018). National population projections [Dataset]. University of Virginia, Weldon Cooper Center, Demographics Research Group. Retrieved from https://demographics.coopercenter.org/national-population-projections

Voisin, N., Kintner-Meyer, M., Skaggs, R., Nguyen, T., Wu, D., Dirks, J., et al. (2016). Vulnerability of the US western electric grid to hydro-climatological conditions: How bad can it get? *Energy*, *115*, 1–12. https://doi.org/10.1016/j.energy.2016.08.059

Wiser, R., Mills, A., Seel, J., Levin, T., & Botterud, A. (2017). *Impacts of variable renewable energy on bulk power system Assets, pricing, and costs*. Lawrence Berkeley National Lab. (LBNL). https://doi.org/10.2172/1411668

Woo, C. K., Olson, A., Chen, Y., Moore, J., Sclag, N., Ong, A., & Ho, T. (2017). Does California's CO_2 price affect wholesale electricity prices in the Western U.S.A. *Energy Policy*, *110*, 9–19. https://doi.org/10.1016/j.enpol.2017.07.059